Electronic Supporting Information

Predicting two-dimensional pentagonal transition metal monophosphides for efficient electrocatalytic nitrogen reduction

Yiran Ying[a], Ke Fan[a], Xin Luo[a,b], and Haitao Huang*[a]*

[a] Department of Applied Physics, The Hong Kong Polytechnic University, Hung Hom, Kowloon, Hong Kong, P.R. China

Email: aphhuang@polyu.edu.hk

[b] School of Physics, Sun Yat-sen University, Guangzhou, Guangdong Province, P.R. China, 510275

Email: luox77@mail.sysu.edu.cn

Table S1. Summary of lattice constant a, bond length d_1, d_2, and bond angle α, β, γ (see Fig. 1a) for penta-MP (M=Ti, Zr, Hf).

	Penta-TiP	**Penta-ZrP**	**Penta-HfP**
$\boldsymbol{a}$ **(Å)**	5.891	6.379	6.302
$\boldsymbol{h}$ **(Å)**	2.264	2.267	2.281
$\boldsymbol{d_1}$ **(Å)**	2.457	2.614	2.589
$\boldsymbol{d_2}$ **(Å)**	2.872	3.148	3.131
$\boldsymbol{\alpha}$ **(°)**	105.26	105.10	104.83
$\boldsymbol{\beta}$ **(°)**	77.75	79.17	78.81
$\boldsymbol{\gamma}$ **(°)**	115.92	119.23	118.75

Table S2. Summary of in-plane elastic constants, Young's moduli Y, Poisson's ratios *v* along *x* (<100>) and diagonal (<110>) direction, and average Bader charge transfer per atom between M and P for penta-MP (M=Ti, Zr, Hf).

	Penta-TiP	**Penta-ZrP**	**Penta-HfP**
C_{11}/C_{22} (N/m)	70.26	80.52	76.48
C_{12} (N/m)	33.59	36.36	41.12
C_{66} (N/m)	37.93	41.67	34.82
Y(x) (N/m)	54.20	64.10	54.37
Y(diag) (N/m)	87.68	97.30	87.48
ν(x)	0.478	0.452	0.538
ν(diag)	0.156	0.168	0.256
Charge transfer	0.34	0.67	0.68

Table S3. DFT-calculated total energy for gases E_{DFT}, zero point energy E_{ZPE}, entropic contribution term TS, and Gibbs free energy G for H_2, N_2, and NH_3 in their gas phases with PBE functional. Values of TS for gases under T=298.15 K are extracted from CRC handbook.[1] Entropic contribution term for adsorbates is neglected and no thermal corrections are taken into account in calculations of G.[2, 3] Since pH values do not change the calculated overpotentials for NRR,[4, 5] we only consider pH=0 in this work for convenience.

Adsorbates	**E_{DFT} (eV)**	**E_{ZPE} (eV)**	**TS (eV)**	**G (eV)**
H_2	-6.767	0.269	0.404	-6.902
N_2	-16.636	0.151	0.592	-17.077
NH_3	-19.536	0.939	0.596	-19.193

Table S4. Zero point energy E_{ZPE} (eV) for all adsorbates in the nitrogen reduction reaction process for penta-TiP, penta-ZrP, and penta-HfP calculated from the vibrational frequencies obtained through the Hessian matrices. The symbol * denotes the active sites of the catalysts.

Adsorbates	Penta-TiP	Penta-ZrP	Penta-HfP
***N**	0.006	0.006	0.005
***NH**	0.217	0.218	0.218
***NH$_2$**	0.522	0.521	0.526
***N≡N**	0.178	0.177	0.179
***N=NH**	0.390	0.393	0.390
***N−NH$_2$**	0.726	0.700	0.688
***NH=NH**	0.808	0.745	0.746
***NH−NH$_2$**	0.945	1.046	0.943
***NH$_3$**	0.933	0.938	0.943

Zero point energy E_{ZPE} is calculated from vibrational frequencies ω_i:[6]

$$E_{ZPE} = \frac{1}{2}\sum_i \hbar\omega_i$$

Table S5. Entropic contributions TS (eV) under T=298 K for all adsorbates in the nitrogen reduction reaction process for penta-TiP, penta-ZrP, and penta-HfP calculated from the vibrational frequencies obtained through the Hessian matrices. The symbol * denotes the active sites of the catalysts.

Adsorbates	Penta-TiP	Penta-ZrP	Penta-HfP
***N**	0.187	0.187	0.187
***NH**	0.125	0.125	0.125
***NH_2**	0.125	0.125	0.125
***N≡N**	0.021	0.020	0.026
***N=NH**	0.029	0.095	0.091
***N−NH_2**	0.051	0.115	0.138
***NH=NH**	0.069	0.037	0.038
***NH−NH_2**	0.122	0.145	0.123
***NH_3**	0.114	0.109	0.081

For adsorbates, only vibrational entropy is taken into consideration, and TS is calculated as:[2, 4, 6]

$$TS = RT\left\{\sum_i \frac{\frac{\hbar\omega_i}{k_B T}}{\exp\left(\frac{\hbar\omega_i}{k_B T}\right) - 1} - \sum_i \ln\left[1 - \exp\left(-\frac{\hbar\omega_i}{k_B T}\right)\right]\right\}$$

where k_B and R represent Boltzmann constant and gas constant, respectively.

Table S6. DFT-calculated total energy E_{DFT} (eV) for adsorbates in the nitrogen reduction reaction process on the surface of penta-MP (M=Ti, Zr, Hf) with DFT-D3 corrections. The symbol * denotes the active sites on the surface of the catalysts.

Adsorbates	**Penta-TiP**	**Penta-ZrP**	**Penta-HfP**
*	-221.832	-234.786	-298.893
***N**	-231.018	-243.908	-308.352
***NH**	-234.850	-247.974	-312.266
$*NH_2$	-238.789	-252.115	-316.226
***N≡N**	-238.982	-252.214	-316.221
***N=NH**	-242.261	-255.427	-319.678
$*N{-}NH_2$	-246.497	-259.038	-323.343
***NH=NH**	-244.782	-258.792	-322.851
$*NH{-}NH_2$	-249.527	-262.721	-326.985
$*NH_3$	-241.935	-255.117	-319.141

Table S7. DFT-calculated total energy E_{DFT} (eV) for adsorbates in the nitrogen reduction reaction process on the surface of penta-MP (M=Ti, Zr, Hf) and gases with RTPSS functional and DFT-D3 corrections. The symbol * denotes the active sites on the surface of the catalysts.

Adsorbates	Penta-TiP	Penta-ZrP	Penta-HfP
*	-234.379	-80.909	272.526
*N	-245.001	-91.537	261.485
*NH	-248.879	-95.672	257.513
*NH_2	-252.961	-99.897	253.442
*N≡N	-254.308	-101.176	252.258
*N=NH	-257.584	-104.451	248.770
*N−NH_2	-261.871	-108.149	245.011
*NH=NH	-260.176	-107.904	245.525
*NH−NH_2	-265.053	-111.935	241.291
*NH_3	-256.133	-102.943	250.505
N_2	-19.264		
H_2	-7.309		

Table S8. DFT-calculated total energy E_{DFT} (eV) for adsorbates in the nitrogen reduction reaction process on the surface of penta-MP (M=Ti, Zr, Hf) with DFT-D2 corrections. The symbol * denotes the active sites on the surface of the catalysts.

Adsorbates	Penta-TiP	Penta-ZrP	Penta-HfP
*	-221.533	-236.588	-305.145
*N	-230.771	-245.818	-314.771
*NH	-234.627	-249.868	-318.741
$*NH_2$	-238.594	-254.060	-322.790
*N≡N	-238.753	-254.115	-322.686
*N=NH	-242.056	-257.367	-326.227
$*N-NH_2$	-246.293	-261.000	-329.973
*NH=NH	-244.539	-260.780	-329.467
$*NH-NH_2$	-249.336	-264.718	-333.671
$*NH_3$	-241.679	-257.004	-325.682

Table S9. DFT-calculated total energy E_{DFT} (eV) for adsorbates in the nitrogen reduction reaction process on the surface of penta-MP (M=Ti, Zr, Hf) and gases with optB86b-vdW corrections. The symbol * denotes the active sites on the surface of the catalysts.

Adsorbates	**Penta-TiP**	**Penta-ZrP**	**Penta-HfP**
*	-148.551	-165.926	-225.091
***N**	-156.456	-173.781	-233.306
***NH**	-160.152	-177.711	-237.101
$*NH_2$	-163.892	-181.675	-240.888
***N≡N**	-162.935	-180.614	-239.724
***N=NH**	-166.087	-183.749	-243.076
$*N-NH_2$	-170.225	-187.241	-246.629
***NH=NH**	-168.409	-186.981	-246.113
$*NH-NH_2$	-173.091	-190.779	-250.147
$*NH_3$	-166.811	-184.465	-243.583
N_2	-13.680		
H_2	-6.634		

Table S10. Comparison of N_2 adsorption energies (eV) of penta-MP (M=Ti, Zr, Hf) calculated with different functionals and vdW corrections.

System	Penta-TiP	Penta-ZrP	Penta-HfP
PBE+DFT-D3	-0.51	-0.79	-0.69
PBE+DFT-D2	-0.58	-0.89	-0.91
optB86b-vdW	-0.70	-1.01	-0.95
RTPSS+DFT-D3	-0.67	-1.00	-1.00
HSE06	-0.54	-0.87	-0.77

For comparison, we provide PBE+DFT-D2, optB86b-vdW, RTPSS+DFT-D3, and HSE06 calculations of N_2 adsorption energies for penta-MP. The mesh for *k*-points sampling is 3×3×1 and kinetic energy cutoff during the HSE06 calculations is set as 400 eV. We note that there are differences between the N_2 adsorption energies calculated with PBE and RTPSS functionals. According to Garza et al.,[7] a large set of chemisorption energies of H, O, I, NO, and CO on different facets of metals like Pt, Ni, Cu, and Pd calculated with PBE and RTPSS have differences up to 0.3 eV, which is consistent with our results. Compared to other vdW correction methods such as DFT-D2 and vdW-DF (for example, optB86b-vdW), the DFT-D3 vdW correction scheme is predicted to have higher accuracy (close to CCSD(T)) and less empiricism,[8] and is therefore adopted in most parts of our calculations. Further test results of two parameters in our DFT-D3 calculations of penta-HfP+N_2 are shown in Figure S12.

Table S11. Comparison of theoretical NRR overpotentials (eV) of penta-MP (M=Ti, Zr, Hf) calculated with different functionals and vdW corrections.

System	Penta-TiP	Penta-ZrP	Penta-HfP
PBE+DFT-D3	0.56	0.72	0.84
PBE+DFT-D2	0.63	0.78	0.86
optB86b-vdW	0.65	0.79	0.91
RTPSS+DFT-D3	0.52	0.68	0.79
HSE06	0.49	0.64	0.76

For comparison, we also provide PBE+DFT-D2, optB86b-vdW, RTPSS+DFT-D3, and HSE06 calculations of key NRR overpotentials for penta-MP. The mesh for *k*-points sampling is 3×3×1 and the kinetic energy cutoff during the HSE06 calculations is set as 400 eV. The results are also close to that calculated with PBE+DFT-D3, with differences less than 0.1 eV.

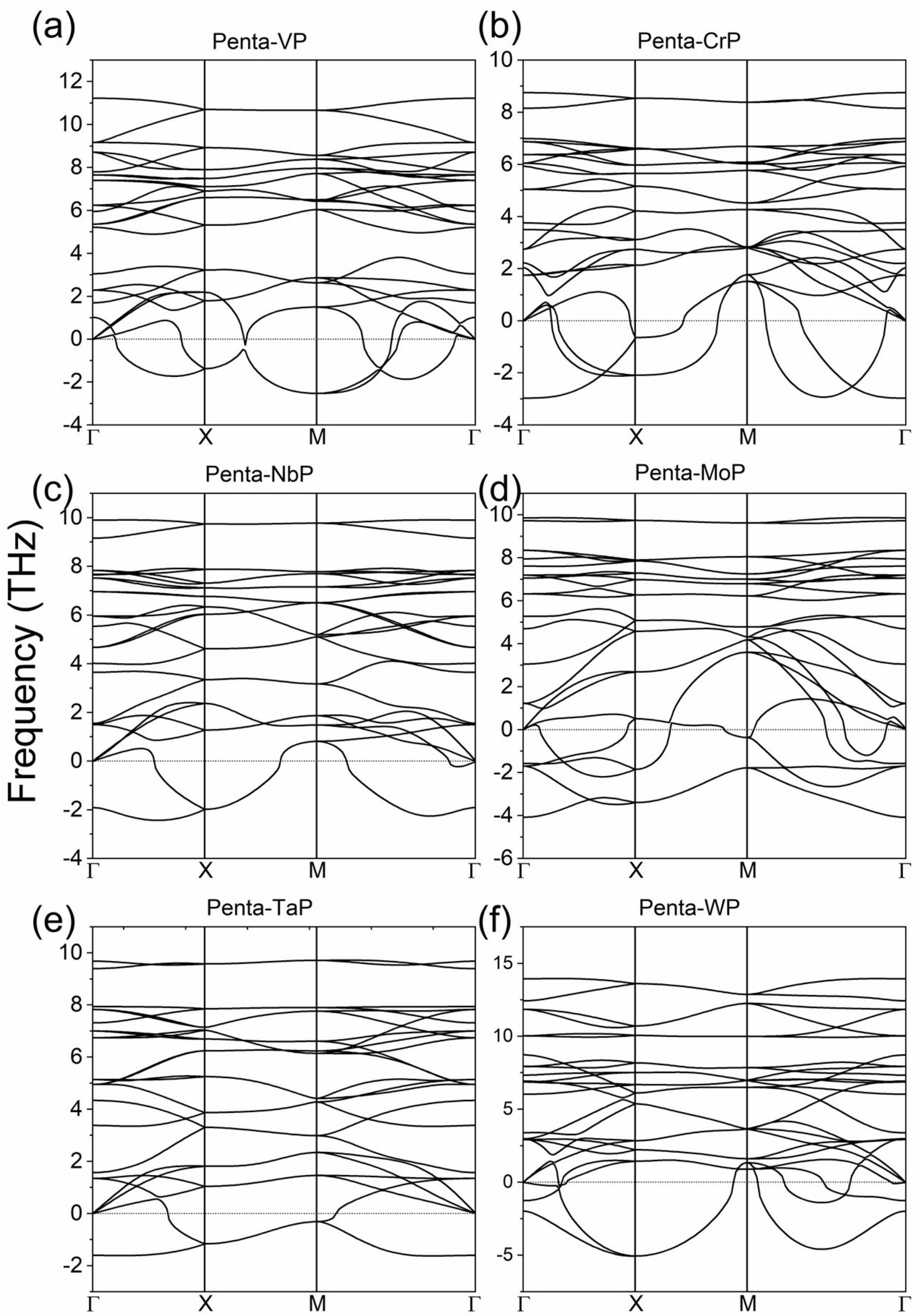

Fig. S1 The phonon dispersion spectra of (a) penta-VP, (b) penta-CrP, (c) penta-NbP, (d) penta-MoP, (e) penta-TaP, and (f) penta-WP.

Orientation-dependent Young's modulus Y(θ) and Poisson's ratio ν(θ) (θ is the angle with respect to x axis) using the following formula:[9, 10]

$$Y(\theta) = \frac{D}{C_{22}\cos^4\theta + \left(\frac{D}{C_{66}} - 2C_{12}\right)\cos^2\theta\sin^2\theta + \sin^4\theta}$$

$$\upsilon(\theta) = \frac{C_{12}\cos^4\theta - \left(C_{11} + C_{22} - \frac{D}{C_{66}}\right)\cos^2\theta\sin^2\theta + C_{12}\sin^4\theta}{C_{22}\cos^4\theta + \left(\frac{D}{C_{66}} - 2C_{12}\right)\cos^2\theta\sin^2\theta + C_{11}\sin^4\theta}$$

here, $D = C_{11}C_{22} - C_{12}^{\ 2}$.

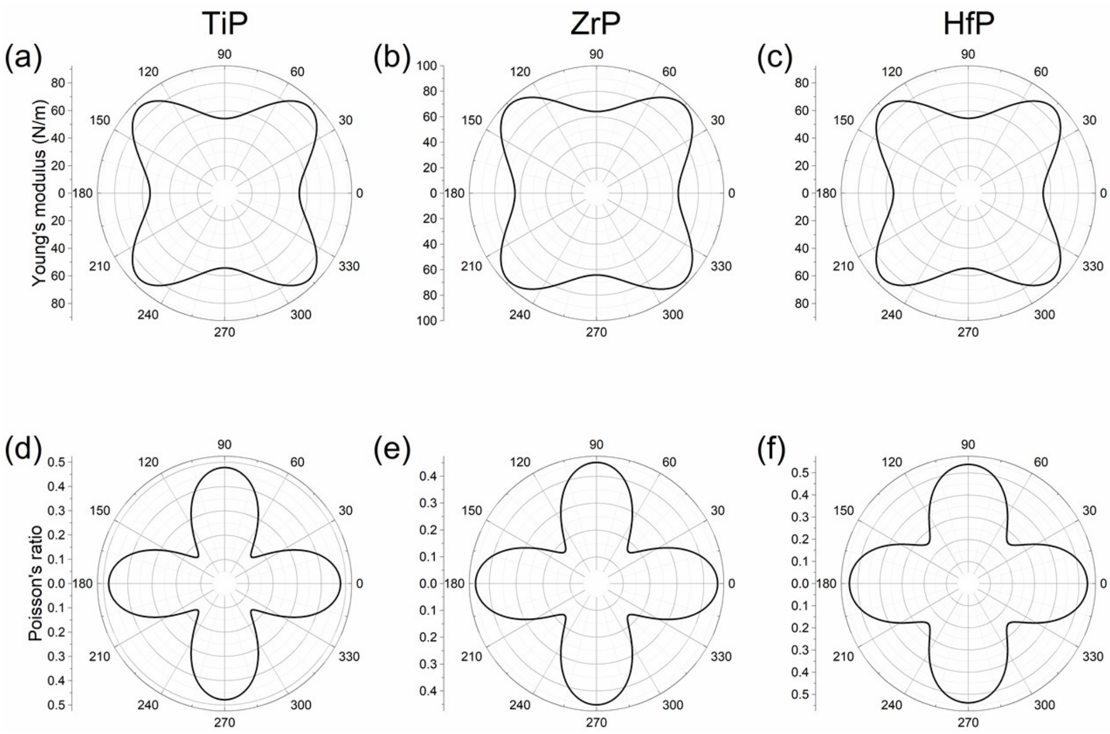

Fig. S2 Orientation-dependent Young's modulus for (a) penta-TiP, (b) penta-ZrP, and (c) penta-HfP, and orientation-dependent Poisson's ratio for (d) penta-TiP, (e) penta-ZrP, and (f) penta-HfP.

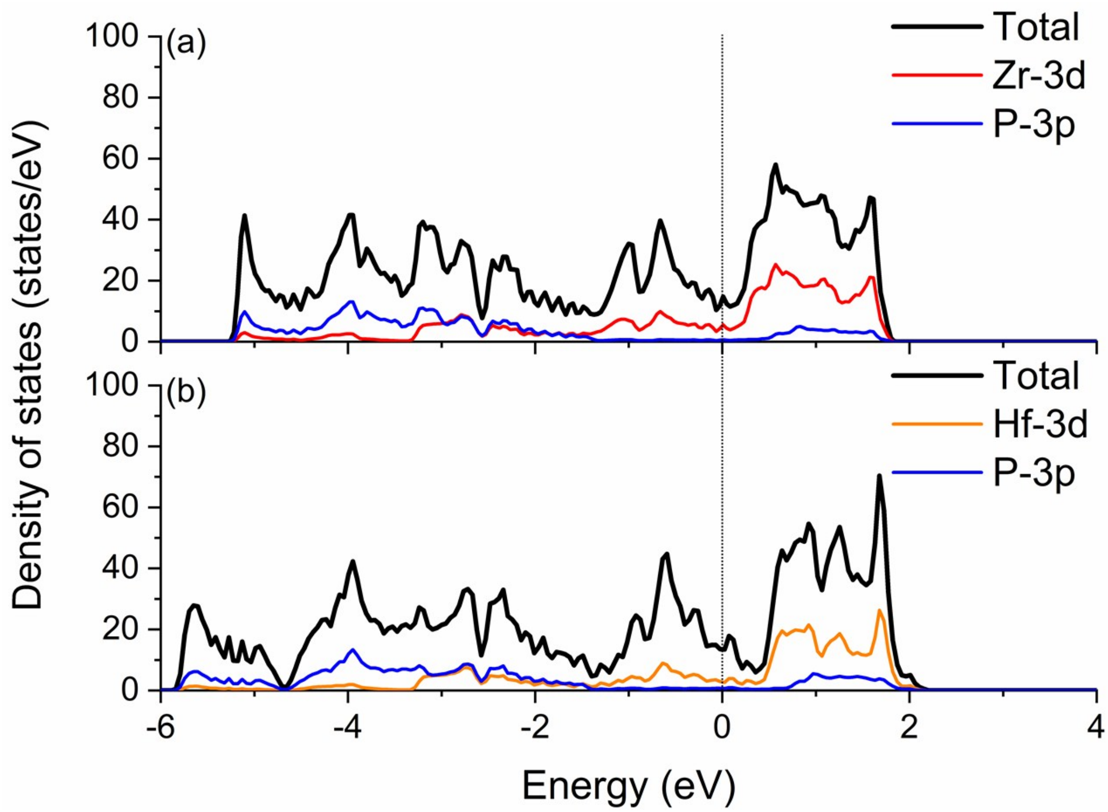

Fig. S3 Total and partial density of states (DOS) for (a) penta-ZrP and (b) penta-HfP. Fermi level is set to zero (denoted by the dotted line).

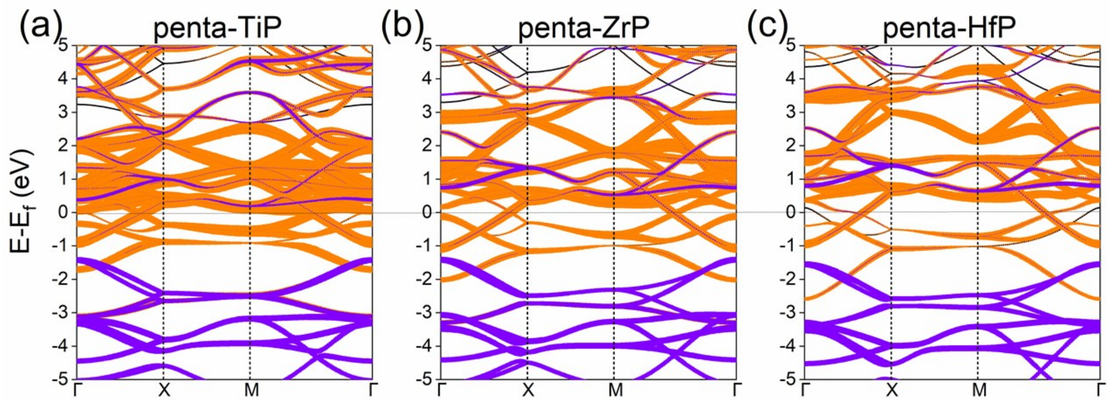

Fig. S4 Characteristic band structures for (a) penta-TiP, (b) penta-ZrP, and (c) penta-HfP. The sizes of the orange and purple dots in the figure are proportional to the weight of the projections of the Ti/Zr/Hf-d state and P-p state, respectively.

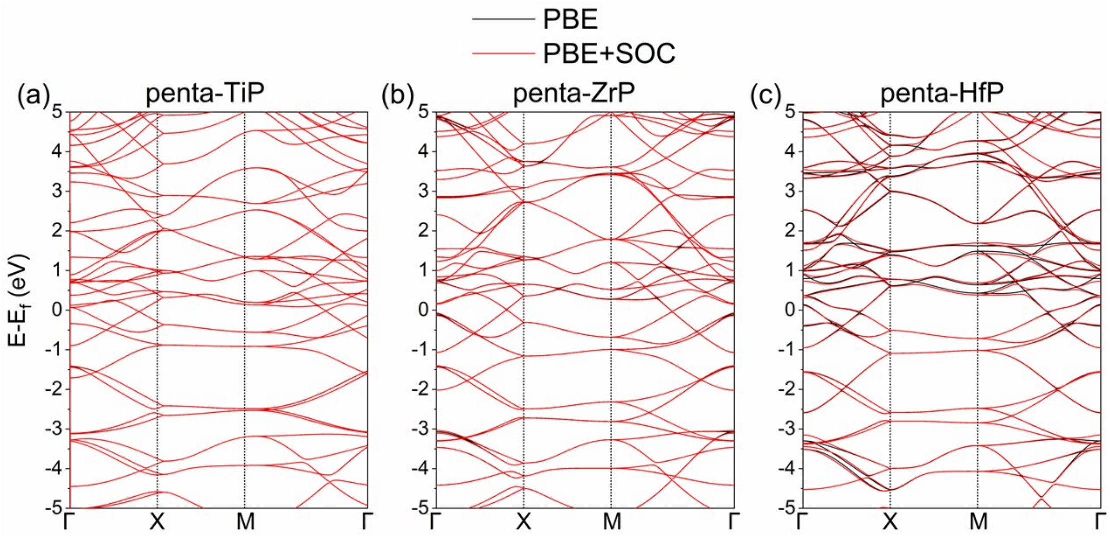

Fig. S5 PBE-calculated band structures for (a) penta-TiP, (b) penta-ZrP, and (c) penta-HfP by excluding (black line) and including (red line) the spin-orbit coupling (SOC) effect.

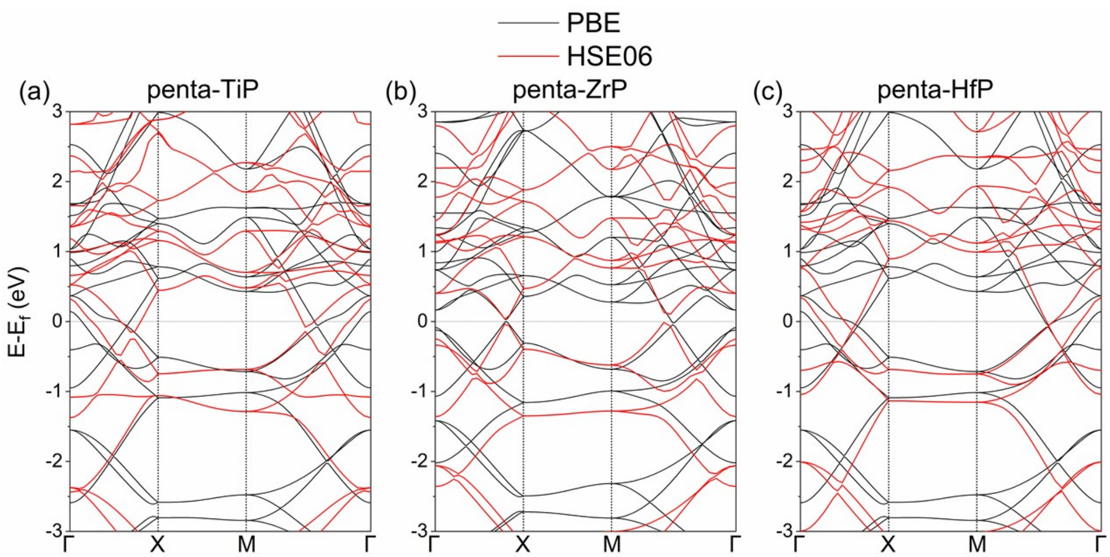

Fig. S6 Band structures for (a) penta-TiP, (b) penta-ZrP, and (c) penta-HfP calculated using PBE (black line) and HSE06 (red line) functionals.

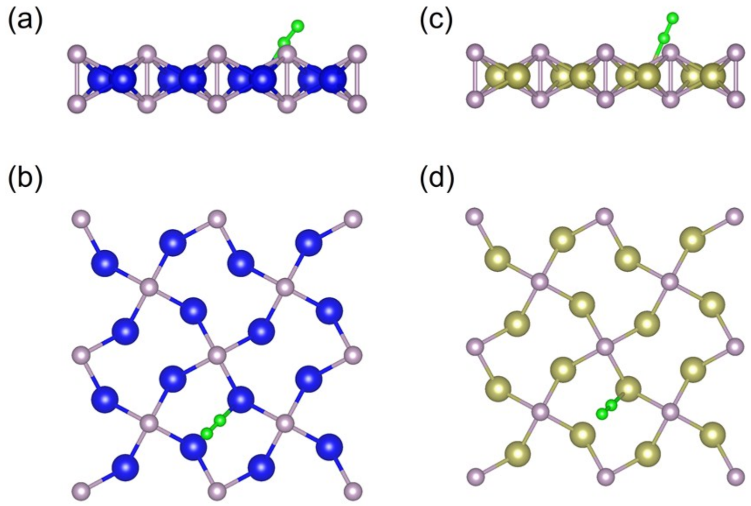

Fig. S7 Top and side view of the crystal structures for one N_2 molecule adsorbed on the 2×2 supercell of (a)(b) penta-ZrP, and (c)(d) penta-HfP.

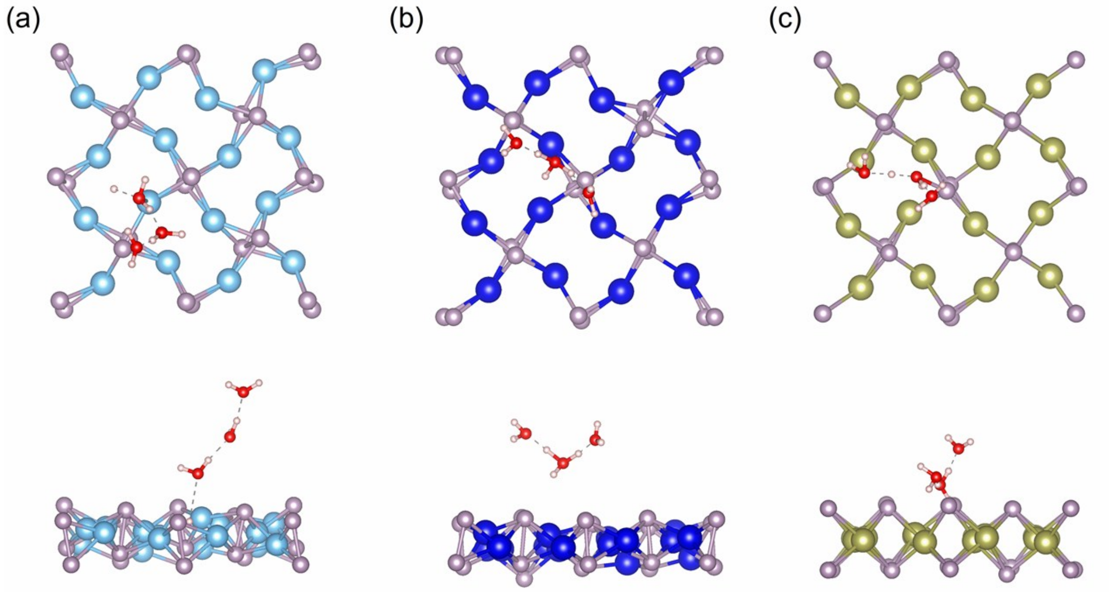

Fig. S8 Snapshots (top and side view) of crystal structure after 5 ps *ab initio* molecular dynamics (AIMD) simulations for (a) penta-TiP, (b) penta-ZrP, and (c) penta-HfP with $(H_2O)_2(H_3O)^+$ cluster in the 2×2 supercell. No obvious structural reconstruction or decomposition can be seen, indicating that penta-MP is stable in aqueous acid solution environment.

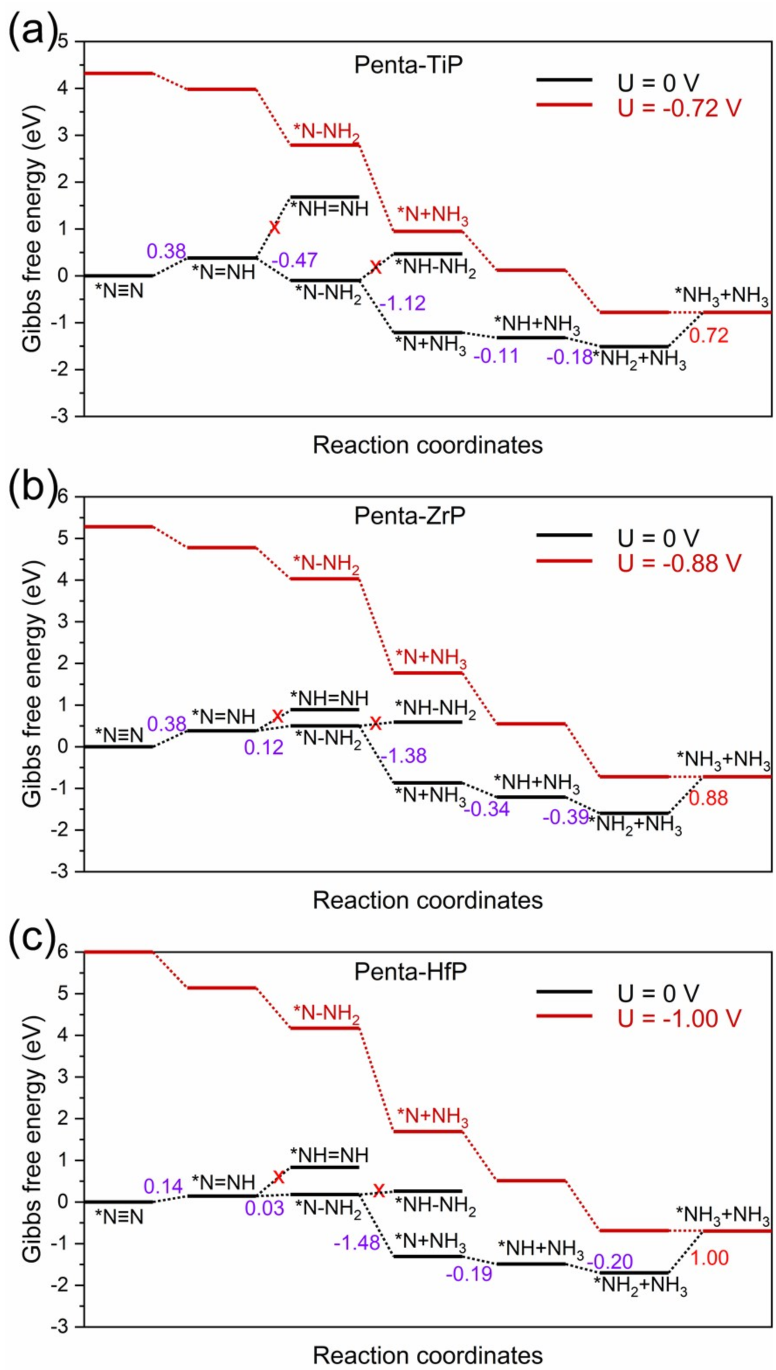

Fig. S9 NRR Gibbs free energy diagrams under zero and applied potential U for (a) penta-TiP, (b) penta-ZrP, and (c) penta-HfP with PBE functional and DFT-D3 corrections. Intermediates with Gibbs free energy changes which are not preferable are marked with red crosses. Relative Gibbs free energy changes for each step under U=0 are marked and shown in the unit of eV.

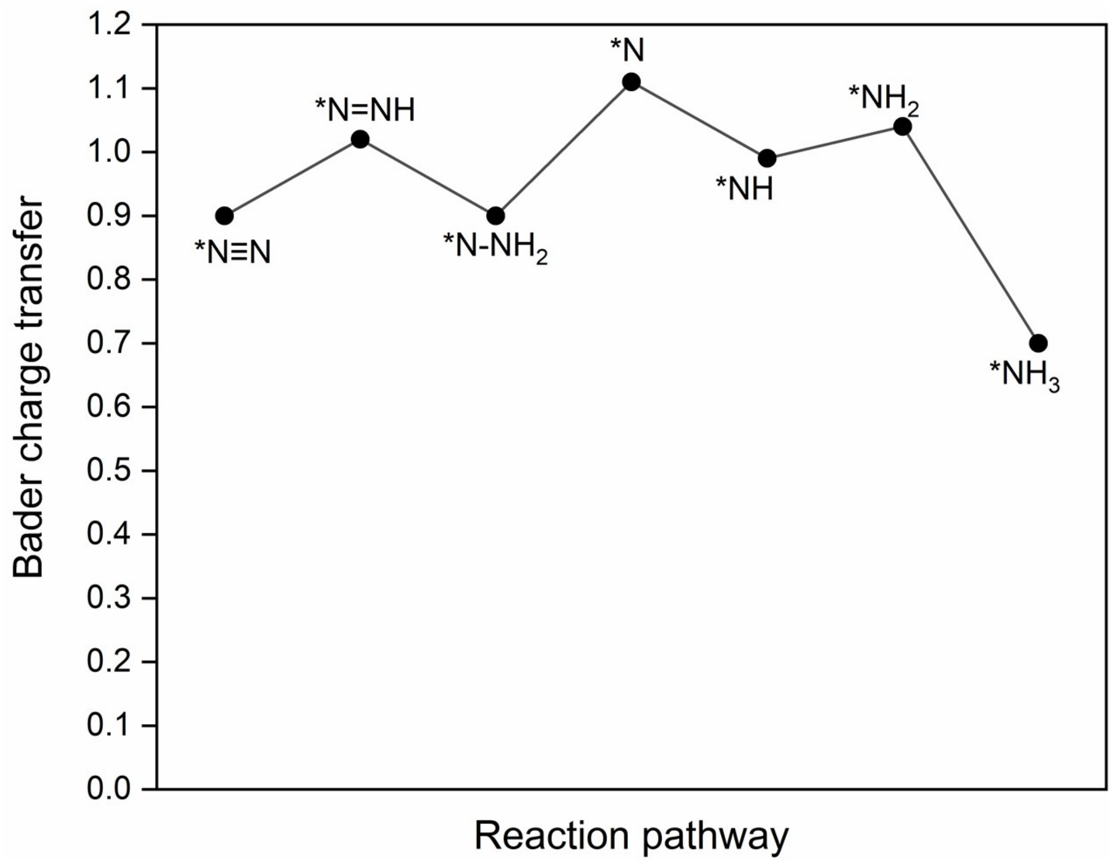

Fig. S10 Variation of Bader charge transfer values between penta-TiP and the adsorbates through the distal NRR pathway.

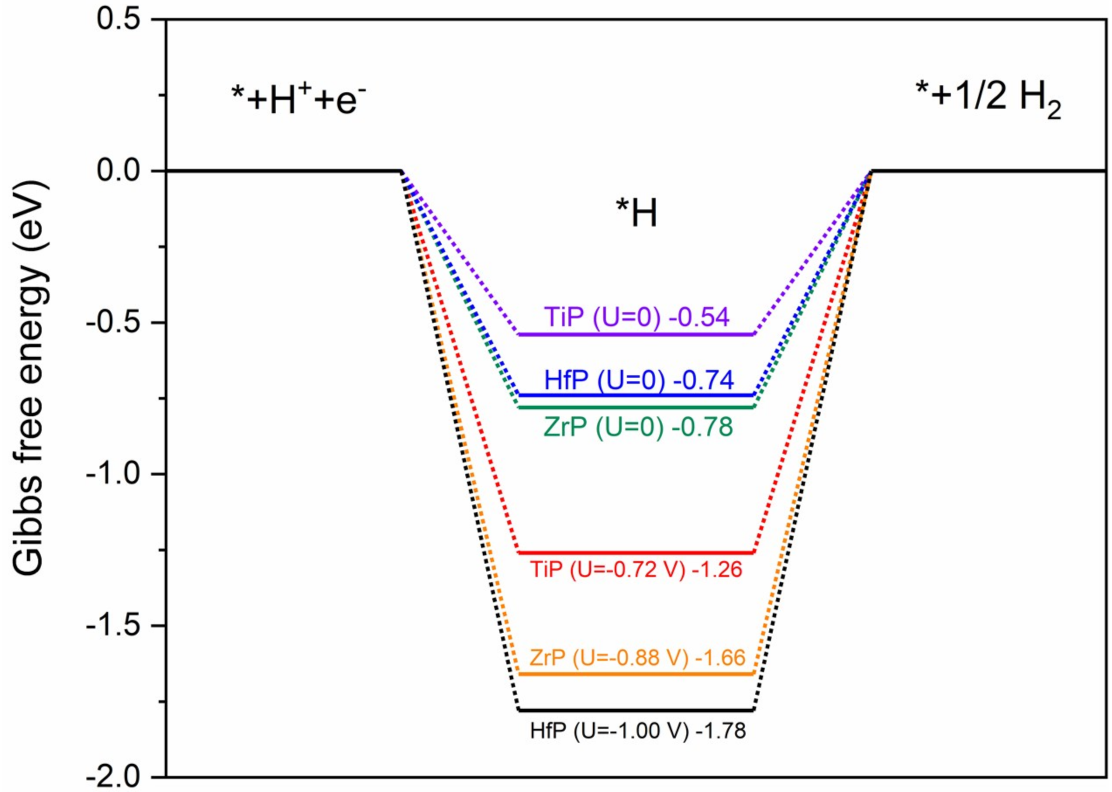

Fig. S11 Single H atom adsorption free energies ΔG_H on penta-MP under zero and applied potential U.

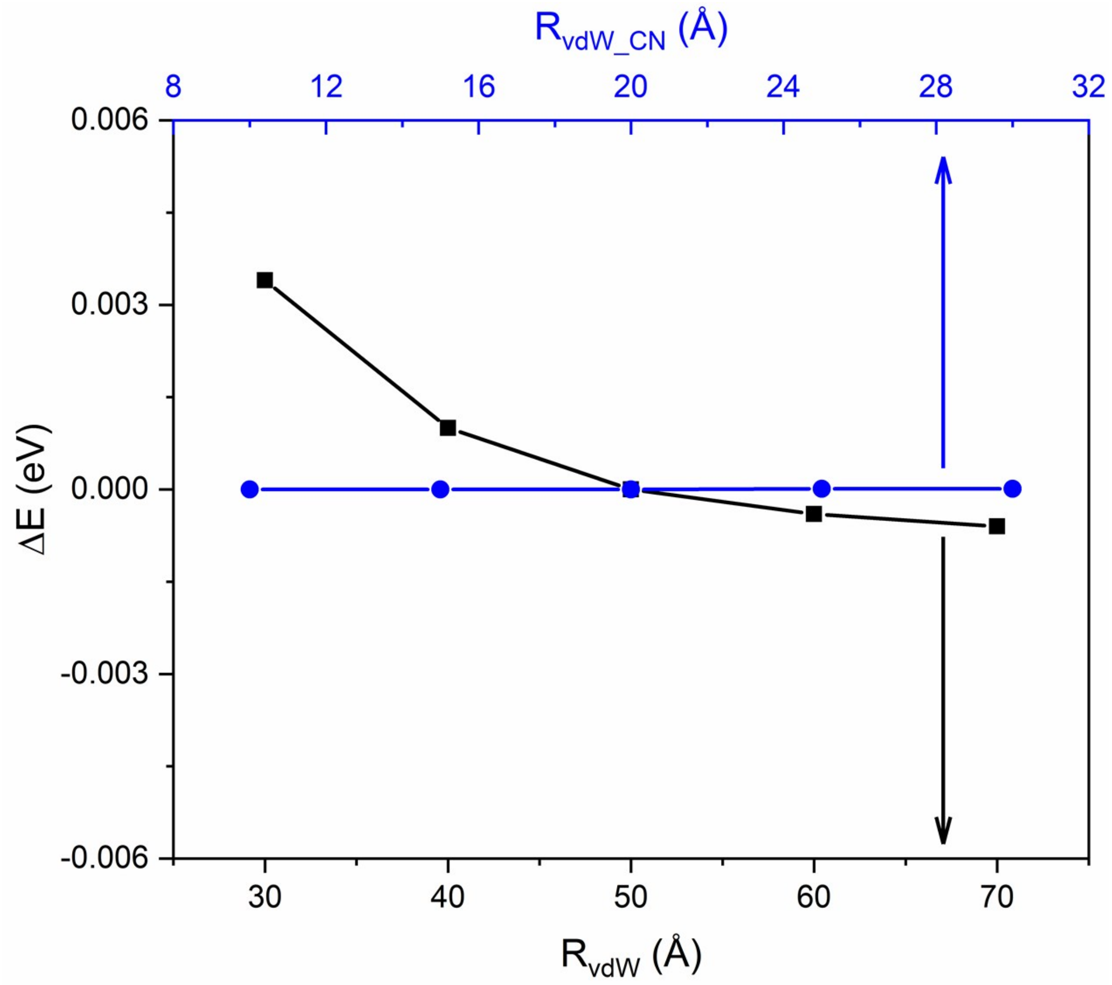

Fig. S12 Test of two parameters in the Grimme's zero-damping DFT-D3 dispersion correction scheme[8] for penta-HfP+N_2, R_{vdW} (cutoff radius for pair interactions) and R_{vdW_CN} (cutoff radius for the calculation of coordination numbers). ΔE denotes relative total energy compared with that calculated under R_{vdW}=50.2 Å and R_{vdW_CN}=20 Å, which are default values in the VASP package and are used in our calculations. We note that maximum total energy difference is only about 0.0034 eV when R_{vdW} is within the range from 30 Å to 70 Å and R_{vdW_CN} is within the range from 10 Å to 30 Å, confirming the validity of parameter choices in our DFT-D3 calculations.

Supplementary references

1. W. M. Haynes, *CRC handbook of chemistry and physics*, CRC press, 2014.
2. L. M. Azofra, N. Li, D. R. MacFarlane and C. Sun, *Energy Environ. Sci.*, 2016, **9**, 2545-2549.
3. M. Bajdich, M. Garcia-Mota, A. Vojvodic, J. K. Norskov and A. T. Bell, *J. Am. Chem. Soc.*, 2013, **135**, 13521-13530.
4. C. Ling, X. Niu, Q. Li, A. Du and J. Wang, *J. Am. Chem. Soc.*, 2018, **140**, 14161-14168.
5. J. Zhao and Z. Chen, *J. Am. Chem. Soc.*, 2017, **139**, 12480-12487.
6. P. W. Atkins, *Atkins' physical chemistry*, Oxford University Press, Oxford, Eleventh edition.. edn., 2018.
7. A. J. Garza, A. T. Bell and M. Head-Gordon, *J. Chem. Theory Comput.*, 2018, **14**, 3083-3090.
8. S. Grimme, J. Antony, S. Ehrlich and H. Krieg, *J. Chem. Phys.*, 2010, **132**, 154104.
9. E. Cadelano, P. L. Palla, S. Giordano and L. Colombo, *Phys. Rev. B*, 2010, **82**, 235414.
10. L. Wang, A. Kutana, X. Zou and B. I. Yakobson, *Nanoscale*, 2015, **7**, 9746-9751.